FLOW FIELD AROUND DIMPLED SHORT PIN-FINS IN A STAGGERED ARRAY

SM Roux*, **GI Mahmood*** , **JP Meyer***
*Department of Mechanical and Aeronautical Engineering, University of Pretoria

Keywords: *pin-fin, dimple, five-hole probe, flow, gas turbine*

Abstract

Flow around cylinders is a widely studied field where the turbulence generating properties are used primarily for heat transfer enhancement. By augmenting the cylinder surface, it is possible to develop additional secondary flows which may increase thermal and hydraulic performance of cylinders. This experimental study looks at the effect that dimples have on the flow behind a pin-fin within a staggered array. The test section consisted of a staggered array of 13 rows of 50 mm pin-fins with 5 pins-fins in each row. The pin-fins had a streamwise spacing X/D and a span-wise spacing S/D of 2. The height ratio H/D was 1.28. A smooth and a dimpled pin-fin configuration was tested. Measurements were taken using a L-shaped five-hole probe between the 10^{th} and 11^{th} row of the array at mid-height for Reynolds numbers of 15 000 and 40 000. The three velocity components and vorticity are analyzed. The results primarily show a decrease in the size and effect of the wake as well as the presence of additional vertical flows.

1 Introduction

Arrays of circular short pin-fins are used in cooling channels of gas turbines, airfoils, combustor liners, electronic chips etc. to enhance the heat transfer and reduce thermal stresses in channel walls. Throughout their history, numerous means of improving their performance have been tested from optimizing pin geometrical relationships to pin augmentation.

Metzger et al. [1, 2, 3, 4], Van Fossen [5] and Simoneau and Van Fossen [6] focused primarily on the effect of pin spacing on the heat transfer and pressure drop as well as developing flow conditions. Heat transfer showed high dependency on the streamwise pin spacing with the closest spaced pins having heat transfer rates twice as high as the most widely spaced array at a Reynolds number of 1 000. This dependency decreased with increasing Reynolds number. Metzger et al.'s correlations [1] are regularly being used for a wide range of pin geometries.

Research was extended to square [7], elliptic [8, 9], and diamond [10] shaped pin-fins which were tested in staggered and inline configurations. Staggered cubic elements [7] showed the most promise with a 30-80% increase in heat transfer over the test range. Goldstein et al. [11] tested pins with stepped diameters which showed a 5% increase in heat transfer. Various other papers were published concentrating on the flow field [9, 12, 13] and heat transfer [13, 14, 15] mechanisms.

Particularly within the last decade, the influence of dimples on fluid flow has become a major research field but most of this research has been focused on plate and channel flow [15, 16, 17, 18]. Results concerning pressure losses have been mixed with some results showing increase and others reduction but the effects of dimples have always been fairly small, therefore, their main attraction appears to be their influence on heat transfer. Kovalenko and Khalatov [19] tested nine configurations of a single row of dimpled pin fins. These pin were varied in terms of dimple size, dimple depth, axial spacing, and angular spacing. Asymmetrical dimples were also tested. They found that shallow, asymmetrical dimpling produced the best results with the best performing configuration resulting in a 70% increase in heat transfer at the highest Reynolds number. This improvement was produced by inducing turbulence at the pin surface and delaying flow separation around the pin.

The purpose of this study is to expand upon the work of Kovalenko and Khalatov [19] by taking their best performing dimple configuration and testing it experimentally, not in a single row, but in a staggered array of pin-fins looking at the effects that dimples have on the fluid flow within a pin-fin array. The analysis of the flow can give a good indication of the expected thermal and hydraulic performance.

2 Experimental Facility

2.1 Wind Tunnel

The experimental facility (Fig. 1) was a suction-type wind tunnel with a rectangular settling-chamber which had a length of ten hydraulic diameters to ensure fully-developed hydrodynamic flow entering into the test section. After the test section was a rectangular-to-round section, an orifice plate and two axial fans, one of which was controlled with a variable speed drive.

The test section (Fig. 2) had an inside width of 500 mm, a height of 64 mm and a length of 1.35 m. Inside the test section were thirteen staggered rows of 50 mm diameter (D) with a height (H) of 64 mm pin-fins with five pin-fins in each row. The centre-to-centre distance (X) between the pin-fins in the streamwise flow direction was 100 mm and the transverse centre-to-centre distance (S) between the pin-fins were also 100 mm. This gave a pin-fin arrangement of X/D and S/D equal to 2 with H/D equal to 1.28.

2.2 Test Section

The entire test section and pin-fins were constructed from Plexiglas. The pin-fins were interchangeable and two sets of pin-fins were used, a set of pin fins which were smooth and a second set with a dimpled surface (Fig. 3). The dimpled pin specifications were adapted from the best performing configuration from [19]. There were seven rows of dimples on each pin, all of which were spaced 9.24 mm apart. The dimples were 5.20 mm in diameter and were machined asymmetrically with an offset of 3.87 mm, this allows the dimples to have a depth of 0.820 mm on the inside edge and zero on the outside edge. Twenty-four dimples were machined in each row (and therefore had a radial spacing of 15°).

2.3 Five-Hole Probe Measurements

Velocity-field measurements were taken with a calibrated Aeroprobe L-shaped five-hole probe having a 1.6 mm tip diameter which was connected to five calibrated 0.3 psi Omega PX138 pressure transducers showing an accuracy within 2 Pa. The five-hole probe was attached to a Velmex 3-axis traverse system which controlled the probe's movement through the testing area. Measurements are performed between the centre pins of the 10th and 11th rows at mid-height. Measurements were taken every 5 mm in the x- and y- directions where possible (Fig. 4). Between ten and twenty measurements are taken at each point at a frequency of approximately 1.5 Hz.

3 Results

The test results are shown in Fig. 5 to 8. All velocity values are scaled related to the same velocity calculated in (5), as shown below in equations (1) to (3) :

$$u* = \frac{u}{U} \tag{1}$$

$$v* = \frac{v}{U} \tag{2}$$

$$w* = \frac{w}{U} \tag{3}$$

and the scaled vorticity is defined in (4) below:

$$\Omega_z = \frac{\omega_z D}{U} \tag{4}$$

where U is the average channel velocity (5):

$$U = \frac{\dot{m}}{\rho A_{channel}} \tag{5}$$

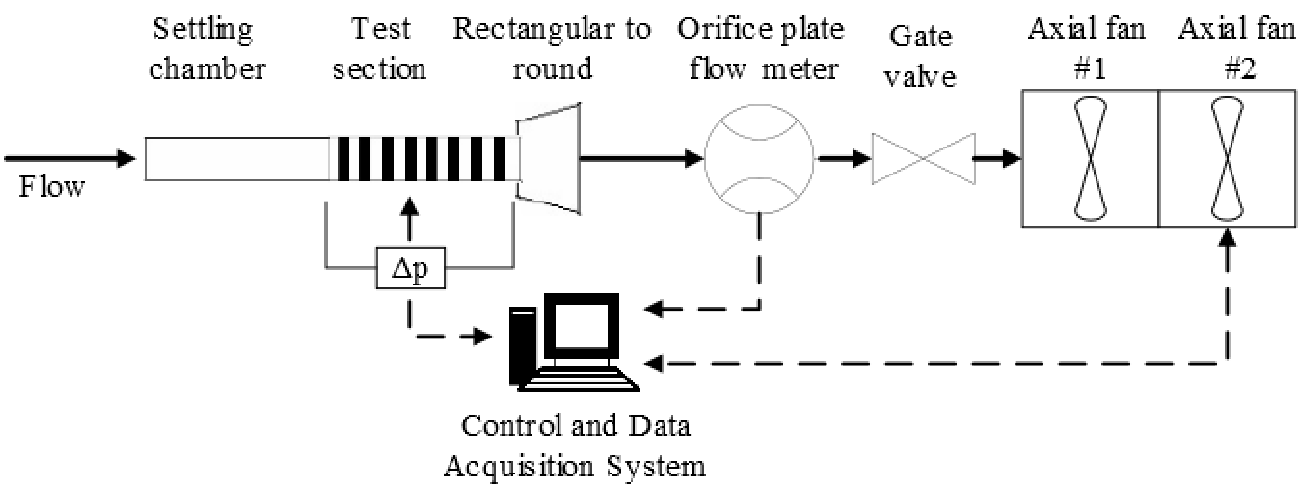

Fig. 1 Schematic of the experimental facility

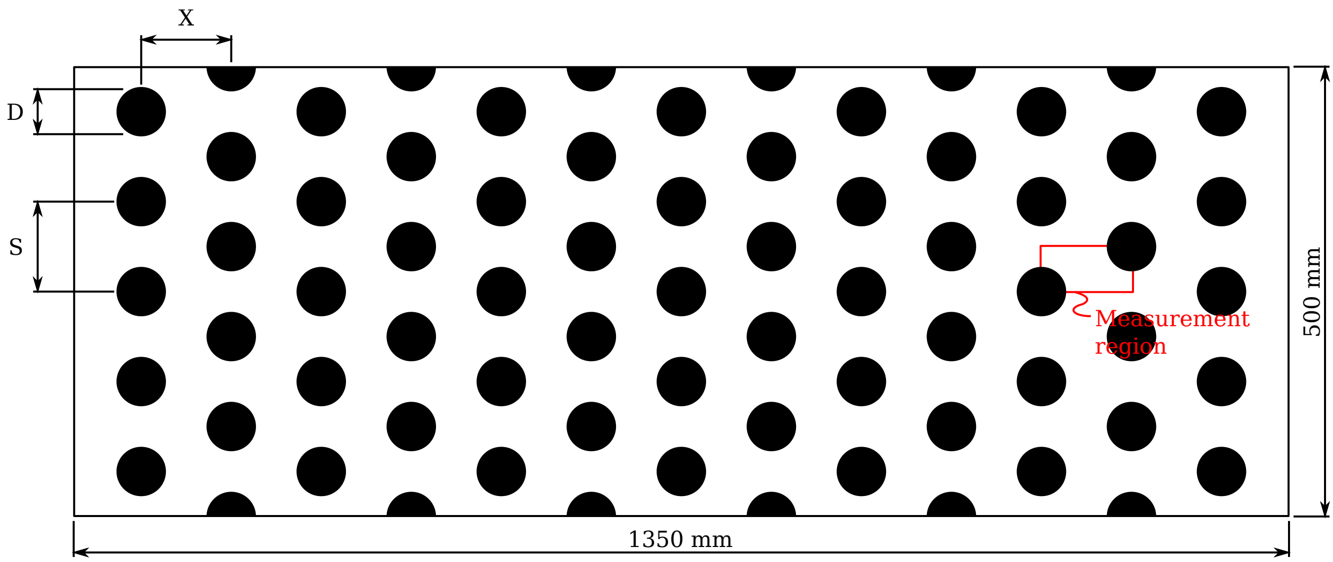

Fig. 2 Schematic of the test section.

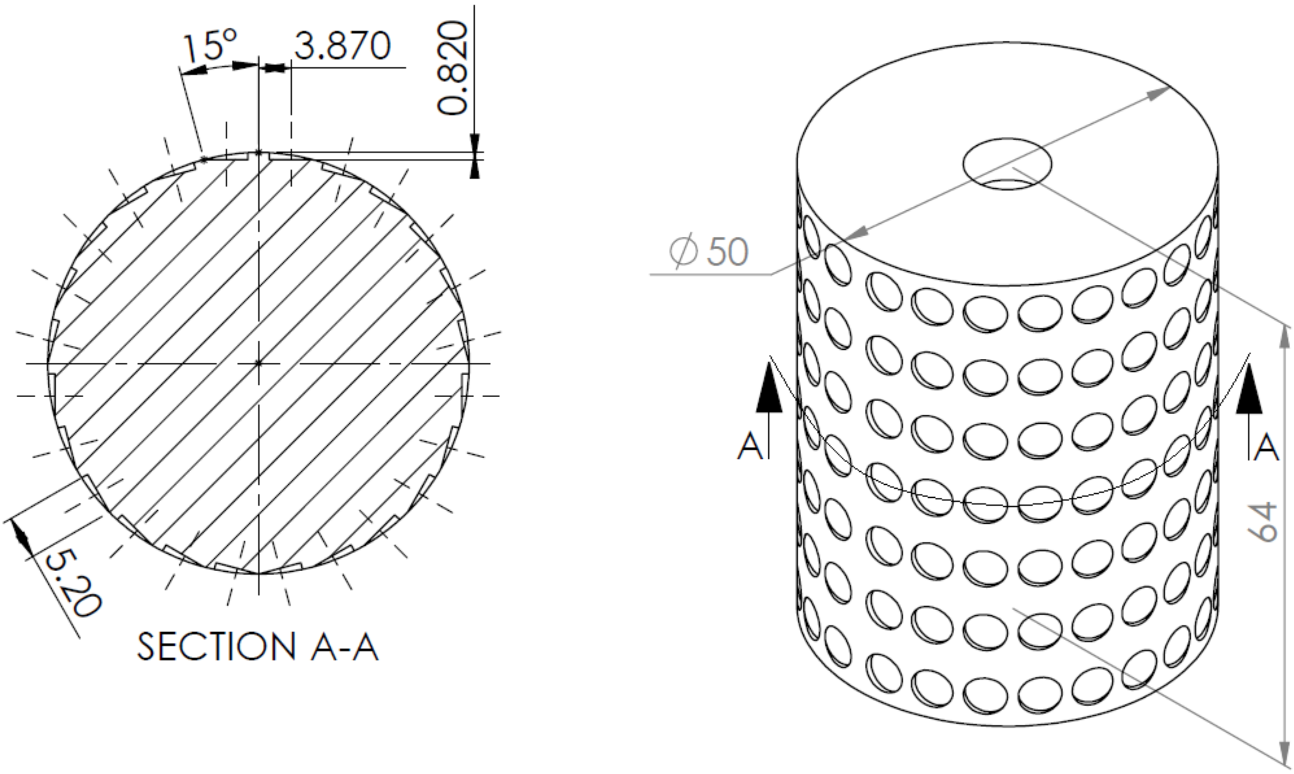

Fig. 3 Dimpled pin parameters. Dimensions are in mm.

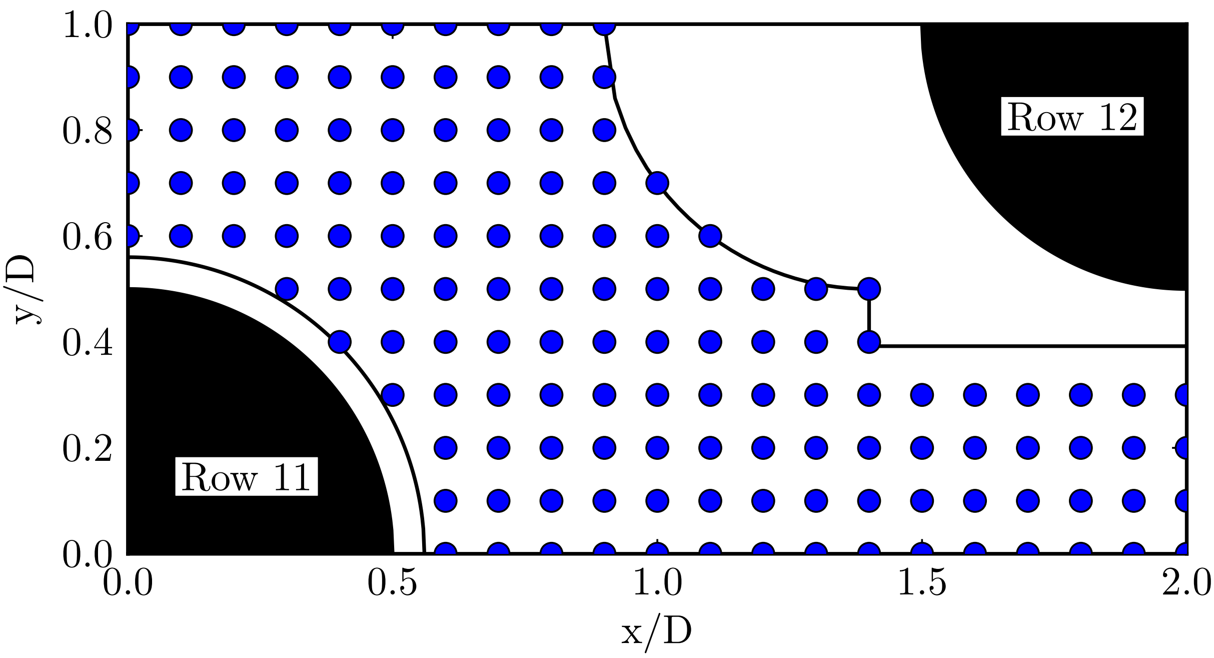

Fig. 4 Five-hole probe measurement grid

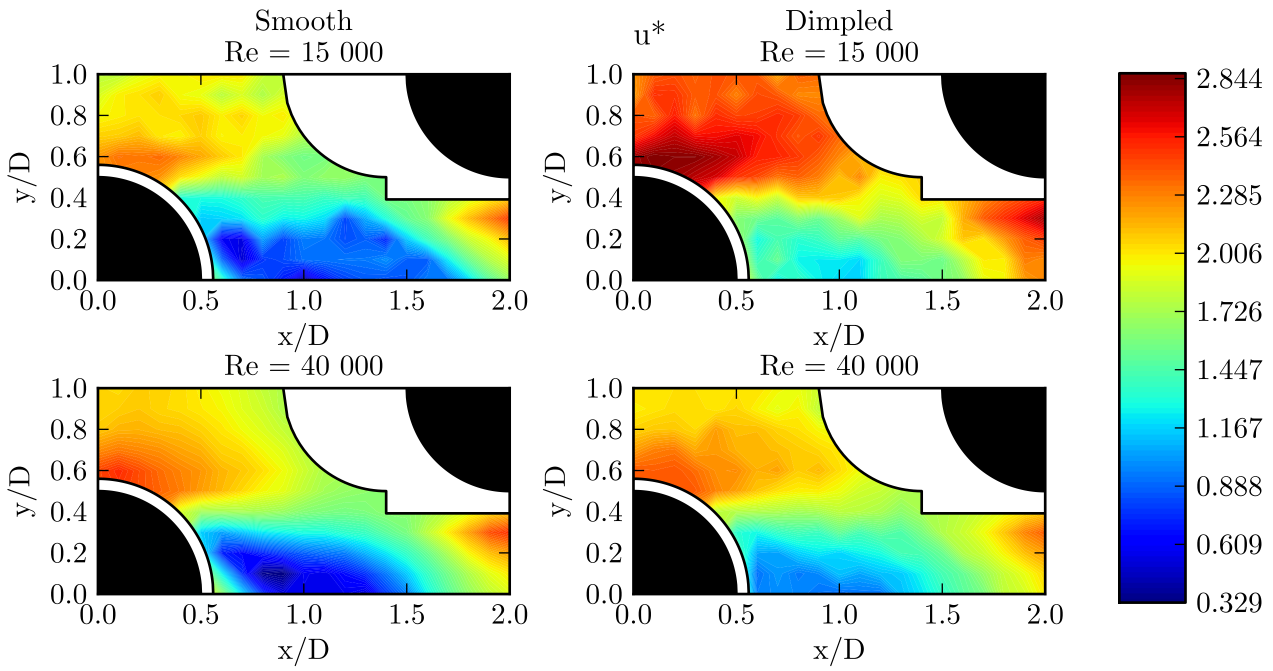

Fig. 5 Scaled streamwise velocity contours

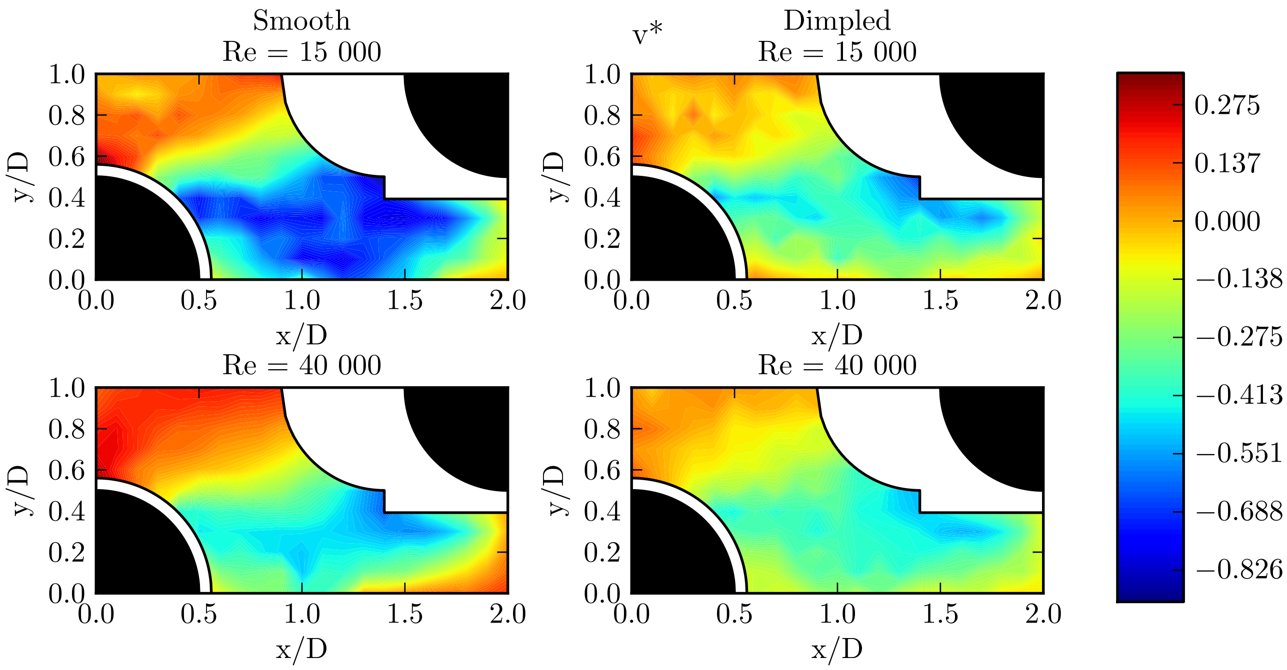

Fig. 6 Scaled spanwise velocity contours

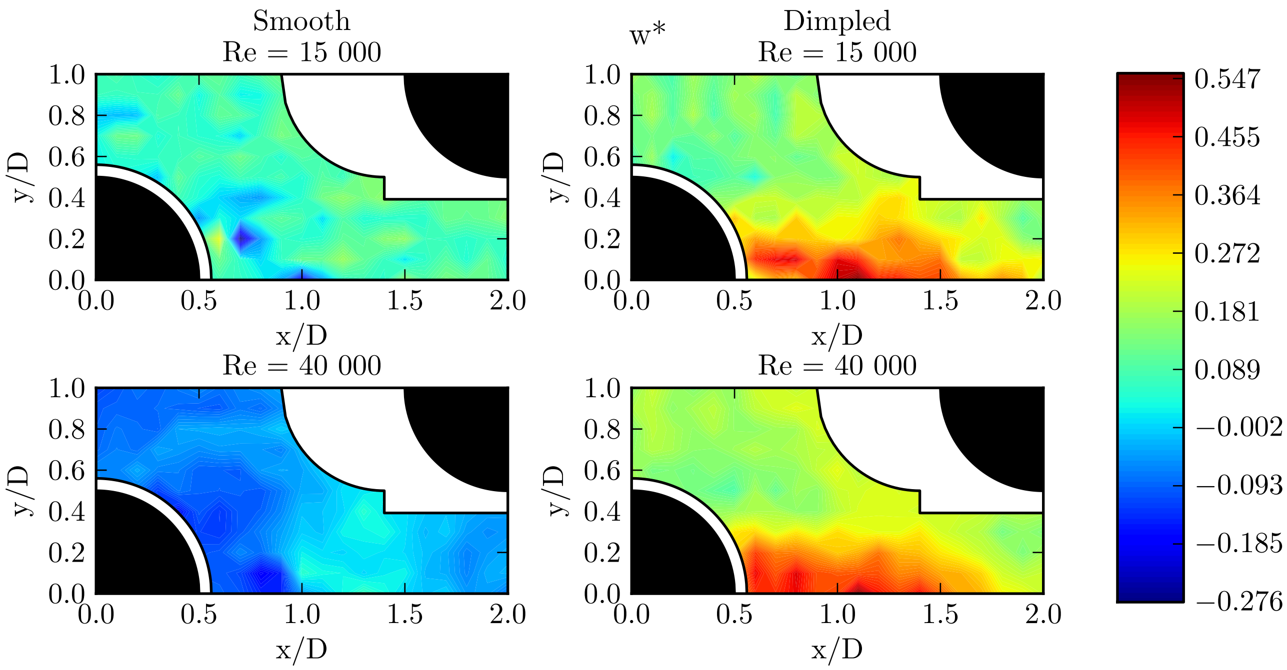

Fig. 7 Scaled vertical velocity contours

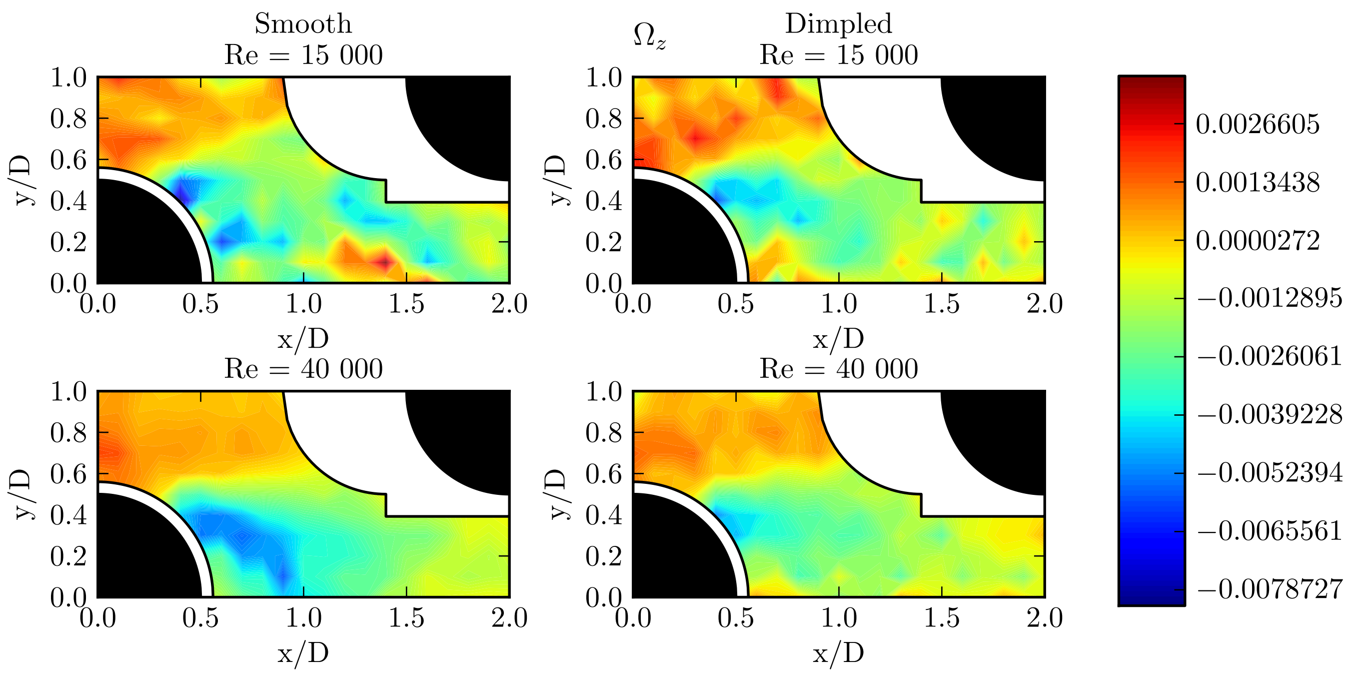

Fig. 8 Scaled vorticity contours

3.1 Streamwise Velocity

The streamwise velocity contours (Fig. 5) for the four test cases are similar with the main difference lying in the wake region. The wakes appear to be equally sized but the difference in the drop of the streamwise velocity is significant with the smooth data showing a drop in u^* to around 0.3 but the dimpled data only drops to around 1.0. The increased wake velocity produced by the dimples could potentially reduce pressure losses and also increase the heat transfer on the endwall since this low velocity region will be removed.

3.2 Spanwise Velocity

The spanwise velocity contours (Fig. 6) add additional insights to the points made concerning the streamwise velocity. The most notable difference is the change in the smooth data between Re = 15 000 and 40 000 in the wake region. The scaled spanwise velocity is significantly larger at the lower Reynolds number which is most likely due to the additional freedom given to the flow due to less pressure from the required high flow rate. There is very little difference between the two dimpled datasets. This reveals that the dimples produce the positive effect of increasing Reynolds number, namely, a reduction in the wake size, at lower Reynolds numbers.

3.3 Vertical Velocity

The vertical velocity contours (Fig. 7) are somewhat more difficult to interpret due to the inability to determine three-dimensional flow patterns from a single horizontal plane. All four plots show a degree of alternating vertical flows pattern in the bulk-flow region, with the smooth data at Re = 40 000 showing the smallest variation. The smooth data also shows fairly little vertical flow variation in the wake region. This differs markedly with the dimpled data which shows very high vertical components in the wake. It is not possible to accurately determine what flow structure this is a part of but it may indicate additional vortical structures developed by the dimples.

3.4 Vorticity

The vorticity contours are shown in Fig. 8 All four sets of data show fairly equivalent vortical magnitudes and also indicate that the separation point for all four are at the same point. For the smooth data, the Re = 40 000 results show a more clearly defined wake region than at Re = 15000 since the boundary is clearly shown by the vorticity contours. Similar to the streamwise velocities, there is very little difference between the two dimpled results once again showing that the dimples appear to reduce the influence of the Reynolds number on the flow.

4 Conclusion

The flow field was measured in an array of smooth and dimpled short pin-fins for Reynolds numbers of 15 000 and 40 000 to determine the effect of dimples. The results show that dimples:

- increase the streamwise flow in the wake.
- reduce the effect of the Reynolds number on flow characteristics.
- induce additional vortical flows.

Dimpled short pin-fins could therefore have a positive influence on both the thermal and hydraulic performance of short pin-fin arrays, particularly at lower Reynolds numbers.

Acknowledgements

This work was supported by the Advanced Engineering Centre of Excellence, NRF, TESP solar hub between UP and SU, EEDSM Hub and the Ballast Project sponsored by the South African Department of Defence and managed by the CSIR.

References

[1] Metzger DE, Fan ZX and Shepard WB. Pressure loss and heat transfer through multiple rows of short pin fins. *Proc. of the Seventh International Heat Transfer Conference*, 1982.

[2] Metzger DE, Berry RA and Bronson JP. Developing heat transfer in rectangular ducts with staggered arrays of short pin fins. *Trans. of the ASME*, Vol. 104, pp 100-706, 1982.

[3] Metzger DE, Fan CS and Haley SW. Effects of pin shape and array orientation on heat transfer and pressure loss in pin fin arrays *Trans. of the ASME"*, Vol. 106, pp 252-257, 1984

[4] Metzger DE, Shepard WB and Haley SW. Row resolved heat transfer variations in pin-fin arrays including effects of non-uniform arrays and flow convergence. *ASME Paper No. 86-GT-132*, 1986.

[5] VanFossen GJ. Heat-transfer coefficients for staggered arrays of short pin fins. *Trans. of the ASME*, Vol. 104, pp 268-274, 1982.

[6] Simoneau RJ and VanFossen GJ. Effect of location in an array on heat transfer to a short cylinder in crossflow. *Trans. of the ASME*, Vol. 106, pp 42-48, 1984.

[7] Chyu MK, Hsing YC and Natarajan V. Convective heat transfer of cubic fin arrays in a narrow channel. *Trans. of the ASME*, Vol. 120, pp 362-367, 1998.

[8] Li Q, Chen Z, Flechtner U and Warnecke H-J. Heat transfer and pressure drop characteristics in rectangular channels with elliptic pin fins. *Int. J. Heat Mass Transfer*, Vol. 19, pp 245-250, 1998.

[9] Uzol O and Camci C. Elliptical pin fins as an alternative to circular pin fins for gas turbine blade cooling applications. *ASME Paper No. 2001-GT-181*, 2001.

[10] Tanda G. Heat transfer and pressure drop in a rectangular channel with diamond-shaped elements. *Int. J. Heat Mass Transfer*, Vol. 44, pp 3529-3541, 2001.

[11] Goldstein RJ, Jabbari MY and Chen SB. Convective mass transfer and pressure loss characteristics of staggered short pin-fin arrays. *Int. J. Heat Mass Transfer*, Vol. 37, pp 149-160, 1994.

[12] Ames FE, Dvorak LA and Morrow JM. Turbulent augmentation of internal convection over pins in staggered pin fin arrays. *J. Turbomach*, Vol. 127, pp 183-190, 2005.

[13] Won SY, Mahmood GI and Ligrani PM. Spatially-resolved heat transfer and flow structure in a rectangular channel with pin fins. *Int. J. Heat Mass Transfer*, Vol. 47, pp 1731-1743, 2004.

[14] Chang SW, Yang TL, Huang CC and Chiang KF. Endwall heat transfer and pressure drop in rectangular channels with attached and detached circular pin-fin array. *Int. J. Heat Mass Transfer*, Vol. 51, pp 5247-5259, 2008.

[15] Rao Y, Wan C, Xu Y and Zhang S. Spatially-resolved heat transfer characteristics in channels with pin fin and pin fin-dimple arrays. *Int. J Thermal Sciences*, Vol. 50, pp 2277-2289, 2011.

[16] Mahmood GI and Ligrani PM. Heat transfer in a dimpled channel: combined influences of aspect ratio, temperature ratio, Reynolds number, and flow structure. *Int. J. Heat Mass Transfer*, Vol. 45, pp 2011-2020, 2002.

[17] Elyyan MA, Rozati A and Tafti DK. Investigation of dimpled fins for heat transfer enhancement in compact heat exchangers. *Int. J. Heat Mass Transfer*, Vol. 51, pp 2950-2966, 2008.

[18] Lienhart H, Breuer M and Köksoy C. Drag reduction by dimples? - A complementary experimental/numerical investigation. *Int. J. Heat and Fluid Flow*, Vol. 29, pp 783-791, 2008.

[19] Kovalenko GV and Khalatov AA. Fluid Flow and heat transfer features at a cross-flow of dimpled tubes in a confined space. *GT2003-38155*, 2003.

Copyright Statement